Fibril orientation and strength in collagen materials and adaptation to strain

Hannah C. Wells[1], Hanan R. Kayed[1], Katie H. Sizeland[1,2], Susyn J.R Kelly[1], Melissa M. Basil-Jones[1], Richard L. Edmonds[3], Richard G. Haverkamp[1,*]

[1]*School of Engineeing and Advanced Technology, Massey University, Riddet Road, Palmerston North 4410, New Zealand*
[2]*SAXS/WAXS, Australian Synchrotron, 800 Blackburn Road, Clayton, VIC 3168, Australia*
[3]*Leather and Shoe Research Association, Dairy Farm Road, Palmerston North 4414, New Zealand*

DOI: 10.5185/amlett.2018.1844
www.vbripress.com/aml

Abstract

Collagen based soft materials are important as medical materials and as consumer products. Strength is a crucial parameter. A better understanding of the structural factors that contribute to strength is sought. Synchrotron based small angle X-ray scattering was used to characterize the collagen fibril structure and structural arrangement in a range of collagen based materials including leather, surgical scaffold materials and glutaraldehyde stabilized pericardium. Structure was compared with strength and was also characterized during strain. When collagen fibrils are orientated in a highly layered structure (with a high orientation index) the materials exhibit higher tear strength. This applies to leather, surgical scaffolds derived from dermis and pericardium. A more layered structure is found in stronger leather, and depends on the species of the source animal and processing conditions. For surgical scaffolds and stabilized pericardium stronger material is found also to have a more layered structure. In pericardium it is affected by the age of the source animal with younger animals having a more layered fibril arrangement in the pericardium. When collagen based soft materials are strained, the material responds first by a reorientation of the fibrils then by extension of individual fibrils, and this enables them to withstand high stresses.

Keywords: Collagen; leather; orientation; SAXS; structure.

Introduction

Type I collagen is a fibrillar protein that is the major component of many soft tissues in animals **[1]**. These tissues include skin, pericardium, stomach, and tendons. Other types of collagen form important components of bone, cartilage and other organs. In tissues dominated by type I collagen other components are present which contribute to the structure and function of the tissues. These include other collagen types (e.g. type II and III), elastin, and glycoaminoglycans (GAGs) such as dermachondans and hyaluronan. Collagen is essential to the existence of animals by providing structural support and form and performs some of the functions in animals that cellulose does in plants and chitin does in insects. Collagen based soft materials have also been coopted into service in medical materials and consumer products. Examples of these are surgical scaffolds made from decelluarised dermis **[2]**, heart valve leaflets made from pericardium **[3]** and shoes made from leather.

One of the main functions of type I collagen in tissues is to provide structural form. Both strength and elasticity are needed **[4]**. Strength is derived from the fibrillar nature of collagen. Collagen fibrils may be many hundreds of nanometres long, with a diameter in the range 30-100 nm. The fibrils have a high tensile strength along their length. However connections between the fibrils may be less strong. The fibrils are ordered into bundles, which in turn make up fibres. Animal tissues are fibrous materials comprised of these collagen fibres. Strength and elasticity are also important for the technical applications of collagen materials. Strength may be measured in a variety of ways, some of which provide similar information. The methods have often been developed to mimic in-service performance. These include tensile strength **[5]**, tear strength **[6]**, bending stiffness, ball burst test **[7]**, suture pull-out force or stitch tear testing. For leather, tear strength is the most routinely used measure of strength and correlates well with performance in shoes and upholstery. For surgical scaffolds, tear test or the similar ball burst test give information that is relevant to in-service performance. These tests reproduce the normal failure mode of these materials, which is not by catastrophic failure of a large portion of tissue at one time, but rather by a propagating failure at a point stress.

The dynamic properties of tissue and tissue derived materials are also important for their performance. Skin has to stretch and contract to accommodate movement of the body, pericardium has to expand and contract with

each heartbeat, stomach tissue has to expand with each meal. Leather in shoes must flex with each footstep, surgical scaffolds must duplicate the expansion and contraction of the tissue it replaces. Therefore collagen materials must have mechanisms to accommodate this dynamic behavior. These mechanisms may be at the scale of the molecule, fibril, fibre or tissue structure.

The structure of collagen in tissues has been characterized by a range of techniques. Optical microscopy, including staining with picrosirius red, is useful in getting a macroscopic view of the collagen organization **[8]**. Scanning electron microscopy and transmission electron microscopy (TEM) can show the organization of the fibrils and the structure of the fibrils. It has the disadvantages that these methods normally require chemical staining and dehydration which may alter the structure and these methods only show small areas of sample which comes with a risk of not being representative. Atomic force microscopy provides structural information at a similar scale to TEM **[9]** with the similar sampling representation risk, but avoids the need for transformational sample preparation. Small angle X-ray scattering (SAXS) is also useful **[10]** and has advantages over these other techniques in that it may be performed on samples without chemical modification, it can sample a larger volume of sample while providing structural information at a range of scales (e.g. from 1-200nm), and it can be easily and directly quantified **[11]**. SAXS also has the advantage that these measurements can be made while a tissue sample undergoes strain or other mechanical transformations**[12-13]**.

Here the structural aspects of collagen based materials that contribute to strength are investigated. The investigation includes the correlation of measured mechanical properties with nanostructure and also the dynamic changes in collagen structure and structural arrangement under strain. It is hoped that a better understanding of the mechanism of collagen in providing strength and elasticity may both enable manufacture of improved collagen based materials but also provide a better understanding of the performance of natural tissues.

Experimental

Sample source and sample preparation

Leather. The following procedure was used to produce leather from animal skins. Adhering fat and flesh was removed from the skins before a conventional lime sulfide paint (140 g/L sodium sulfide, 50 g/L hydrated lime, 23 g/L pre-gelled starch thickener) was applied to the flesh side of the skin at 400 g/m^3. After an incubation period of 16 h at 20 °C the skins were washed to remove the lime and the pH was lowered to 8 by adding ammonium sulfate. A commercial bate enzyme called Tanzyme (0.1 % w/v) was then added and the skins were held at 35 °C for 75 min before being washed and pickled (20% w/v sodium chloride and 2% w/v sulfuric acid). The pickled skins were then degreased using a 4% nonionic surfactant (Tetrapol LTN, Shamrock, New Zealand) at 35 °C for 90 min before being washed. To neutralize the skins they are then washed for 10 min in 8% NaCl, 1% disodium phthalate solution (Feliderm DP, Clariant, UK) and 1% formic acid. The mix was then made up to 5% chrome sulfate using Chromosal B (Lanxess, Germany) and processed for 30 min. 0.6% magnesium oxide is then added based on the weight of the skins to fix the chrome and is processed over night at 40 °C. The resulting wet-blue pelts are neutralized again, using 1% sodium formate and 0.15% sodium bicarbonate for 1 h. The pelts are then washed and retanned with 2% synthetic retanning agent (Tanicor PW, Clariant, Germany) and 3% vegetable tanning (mimosa; Tanac, Brazil). 6% mixed fatliquors were added and the leathers were held at 50 °C for 45 min, followed by fixing with 0.5% formic acid for 30 min and washing in cold water.

Pericardium. Fresh bull (Charolais Cross) pericardium samples were sourced within 2 h of slaughter from John Shannon, Wairapara, New Zealand. The tissue was cut into rectangular sample pieces (50 mm × 6mm) with the long axis being parallel to the long axis of the heart. The pericardium was washed for 24 h in 1% octylphenol ethylene oxide condensate (Triton X-100, Sigma) and 0.02% EDTA solution made up in phosphate buffered saline (Lorne Laboratories Ltd). Finally, the samples were stored in phosphate buffered saline up until experimental analysis.

Surgical scaffold materials. Commercial acellular dermal matrix (ADM) materials were obtained. These included Strattice Firm porcine ADM (LifeCell Corporation, US), Alloderm human ADM (LifeCell Corporation, US) and a range of SurgiMend bovine ADM (TEI Biosciences, US). The range of SurgiMend bovine ADM included third trimester fetal ADM and neonatal ADM (animals less than 5 months old). Strattice and Alloderm were transported as sterile hydrated materials whereas the SurgiMend materials were transported dry and required hydrating with distilled water prior to SAXS analysis and physical testing.

Synchrotron SAXS

SAXS diffraction patterns were recorded on the SAXS/WAXS beamline at the Australian Synchrotron (Melbourne, Australia). A high-intensity undulator source was used with an energy resolution of 10^{-4} obtained from a cyro-cooled Si(III) double-crystal monochromator. The beam size was 250 × 80 μm (FWHM focused at the sample) with a total photon flux of around 2×10^{12} ph.s^{-1}. Diffraction patters were recorded with an X-ray energy of 12 keV using a Pilatus 1 M detector that had an active area of 170 × 170 mm and a sample-to-detector distance of 3371 mm. Exposure time for diffraction patterns ranged between 1 and 5 s and initial data processing was carried out using Scatterbrain software.

SAXS data was recorded in two directions through the samples. The X-ray beam either passed through the

flat (top) surface of the sample, normal to the surface or edge-on to the sample (referred to as edge-on or cross sections). For edge-on analysis, the structure was analysed every 0.1 – 0.2 mm through the sample, since the structure is known to vary through the thickness.

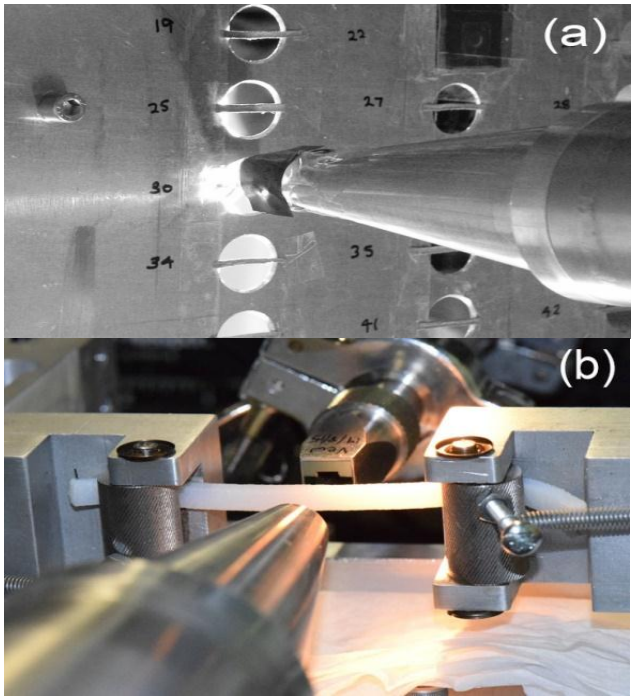

Fig.1. SAXS experimental setup. (a) Samples of leather or tissue mounted for measurement without strain, (b) samples mounted for SAXS measurement during strain. (a) Reprinted with permission from Basil-Jones, M. M. et. al., *J. Agric. Food Chem.* **2010,** *58*, 5286. ©2010 The American Chemical Society.

Samples were strained with apparatus using a linear motor, Linmot PS01 48 _ 240/30_180-C (NTI AG, Switzerland), mounted on a purpose-built frame. Clamps to hold the pericardium were fitted between the linear motor and a L6D OIML single-point loadcell (Hangzhou Wanto Precision Technology Co., Zhejiang, China). Samples were mounted horizontally without tension and strained in 1mm increments and maintained for 1min at each extension to stabilize before SAXS patterns, the extension and the force information were recorded. This process was repeated until the sample failed, with the interval between strain increments around 8–13 min.

Fibril Diameter. The Irena software package, running on Igor Pro, was used to calculate fibril diameters from collected SAXS data. The data were fitted at the wave vector, q, between 0.01 – 0.04 $Å^{-1}$ and at an azimuthal angle which was approximately 90° to the long axis of most of the collagen fibrils. The long axis of most of the collagen fibrils was determined as the azimuthal angle that had the maximum intensity for the D-spacing diffraction peaks. The "cylinderAR" shape model with an arbitrary aspect ratio of 30 was used for all fitting. We did not attempt to individually adjust the aspect ratio for all samples, and the unbranched length of collagen fibrils could in fact exceed this ratio.

Orientation Index. The orientation index (OI) is a measure of the spread of fibril orientation. The spread is quantified to a value between 0 and 1, where 0 indicates isotropically orientated fibrils and 1 indicates parallel fibrils. The OI is defined by the equation (90° – OA)/90°, where OA (orientation angle) is the minimum azimuthal range that contains 50% of the microfibrils, using the spread in azimuthal angle of D-spacing diffraction peaks, converted to an index. The peak area is measured above a fitted baseline, at each azimuthal angle.

Electron microscopy

SEM. To carry out scanning electron microscopy, samples were cut into small cube-shaped pieces and fixed for at least 8 h at room temperature in Modified Karnovsky's fixative. This fixative contains 3% glutaraldehyde and 2% formaldehyde in 0.1 M phosphate buffer (pH 7.2). Following fixing, the samples were washed three times in phosphate buffer (0.1 M, pH 7.2) for 10 – 15 min before being dehydrated in a graded series of ethanol washes (25, 50, 75, 95 and 100%). Each dehydration stage was carried out for 10 – 15 min, and this was followed by a final wash for 1 h with 100 % ethanol. Critical point (CP) drying was carried using the Polaron E3000 series II critical point drying apparatus. Liquid CO_2 was used as the CP fluid and 100% ethanol as the intermediary fluid. The samples were then mounted on to aluminium stubs and sputter coated with gold using the Baltec SCD 050 sputter coater. Samples were viewed in the FEI Quanta 200 environmental scanning electron microscope at an accelerating voltage of 20 kV.

TEM. For transition electron microscopy, samples were fixed with 20 g kg^{-1} formaldehyde and 30 g kg^{-1} glutaraldehyde in 0.1 $molL^{-1}$ phosphate buffer (pH 7.2) for 2 h at room temperature. Samples were washed and fixed with 10 g kg^{-1} OsO_4 in buffer for 1 h at room temperature. After a further three washings for 10 min each, the samples were dehydrated using acetone/water series (150, 500, 750, 950, 1000 g kg^{-1}). Each stage was carried out for 10 – 15 min each and was followed by two pure acetone washes for 1 h each. Samples were first embedded with an acetone resin 50:50 mixture (Procure 812 ProSciTech, Australia), left on a stirrer overnight, then were left for another 8 h in pure acetone and stirred; this step was repeated twice. Lastly, the samples were embedded in pure resin at 60 °C for 48 h.

Atomic Force Microscopy (AFM)

Small square sections of sample were cut and mounted onto 12 mm diameter magnetic metal discs using double-sided tape. Sample were left to air dry for a few h before being imaged. Sample were viewed using a Nanoscope E (Veeco) atomic force microscope with a JV scanner. An x-y calibration to ±3% was completed just prior to imaging. CSG01 cantilevers (NT-MDT, Russia) were used for contact mode imaging, with a force constant of about 0.05 Nm^{-1}.

Optical Imaging with Picrosirius Red Staining

Samples were frozen and cut in a Leica CM1850 UV cryogenic microtome at -30 °C before being mounted on microtome discs using an embedding medium. Cross-sections of samples were cut, each being 10 µm thick, and transferred on to glass microscope slides. The mounted samples were then stained following the procedure given with the Picrosirius Stain Kit (Polysciences, Inc.) and placed in 70% ethanol for 45 s, before being left to air dry for several h. A Nikon Digital Sight DS-Fi2 camera was used to view the samples and collect images with cross-polarised filters.

Tear Tests

Tear strength for each material was determined using standard methods for double-edge tear testing **[6]**. Samples were cut to size and stored at 20 °C and 65 % relative humidity for 24 h before testing. Thickness of each sample was measured prior to testing, using method BS EN ISO 2589:2002. An Instron 4467 was used to carry out the tear tests.

Results and discussion

Images of materials

The structure of ovine dermis (in the form of leather) and pericardium at a range of scales and with a range of imaging techniques are shown in **Fig. 2**. The materials are not of uniform composition throughout, and this reflects the function of the native materials. Leather has a smooth upper surface that forms a barrier to the environment. In leather the top half (approximately) is referred to as grain and this is the portion that formerly contained hair follicles. The lower half is referred to as corium. Similarly in pericardium the internal side is lubricated and slides against the heart with every beat, whereas the external side is the interface with the abdominal cavity. An optical image of a cross section **(Fig. 2a)** demonstrates the gross differences between grain and corium. A stained cross section of pericardium **(Fig. 2b)** highlights the arrangement of collagen in pericardial tissue. At higher magnification the fibrils in bundles can be seen in a SEM image of ovine leather **(Fig. 2c),** with the banding of collagen fibrils in pericardium visible in an AFM image **(Fig. 2d)** or in a TEM image of bovine leather **(Fig. 2e)**.

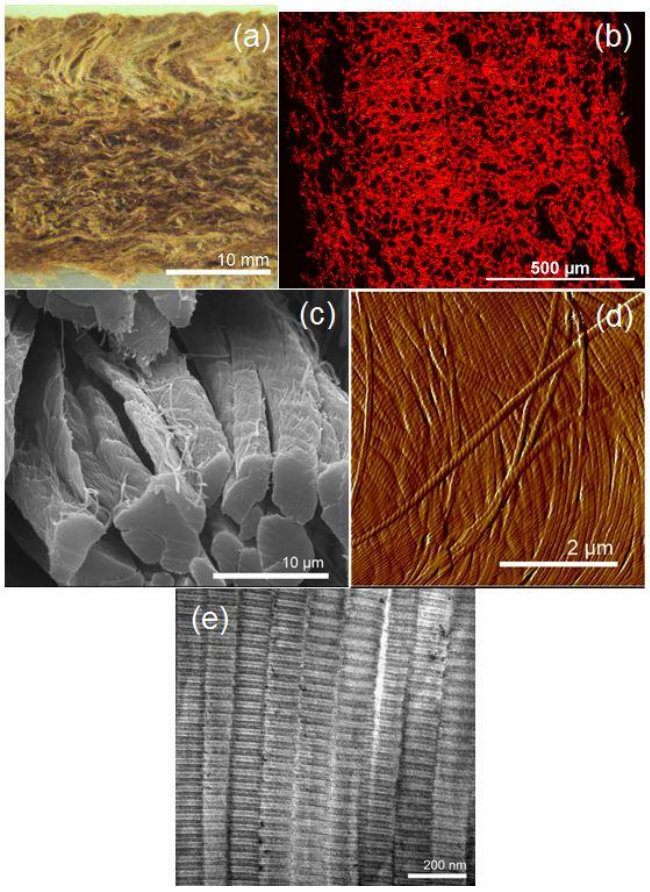

Fig. 2. Tissue imaged with different techniques: (a) optical microscopy of an ovine leather cross section; (b) picrosirius red stained cross polarized optical section of pericardium; (c) scanning electron microscopy of ovine leather; (d) AFM of fresh pericardium; (e) TEM of bovine leather corium.

SAXS patterns

The imaging techniques provide a good insight into the structure of collagen tissues and a variety of scales, however, SAXS provides quantitative information on these structures in a volume averaged sample, although not in such a visually intuitive manner **[11]**. A typical scattering pattern of a collagen material **(Fig. 3a)** gives a series of partially aligned diffraction rings, and a central region of scattering aligned at 90° to the alignment of the diffraction rings. This scattering pattern can be processed

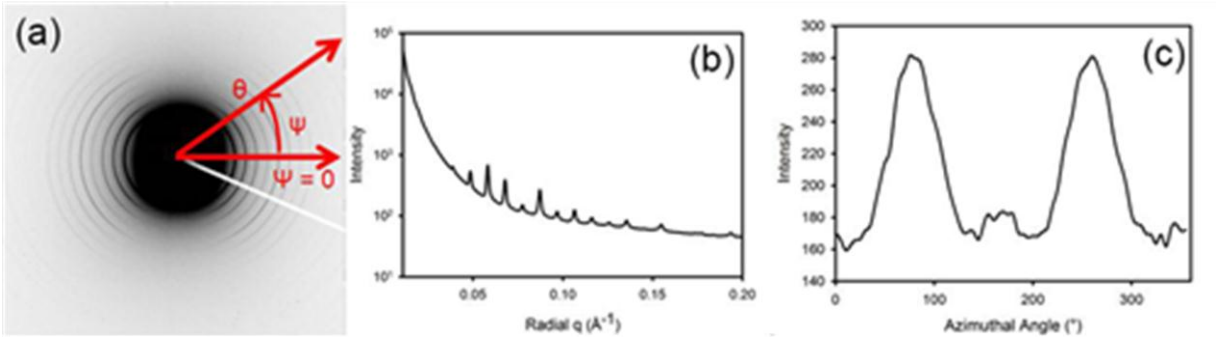

Fig. 3. Representative small angle X-ray scattering. (a) Scattering pattern showing directions of integration for radial, θ, and azimuthal, ψ, angles; (b) intensity with radial angle integrated over all azimuthal angles; (c) intensity with azimuthal angle integrated over a small range or radial angle corresponding to one diffraction ring.

in a variety of ways. Two useful methods are to plot the intensity with radial angle integrated over all azimuthal angles **(Fig. 3b)** or the intensity with azimuthal angle integrated over a small range or radial angle corresponding to one diffraction ring **(Fig. 3c).**

OI and tear strength

The orientation index was measured both with the X-rays edge on to the tissue or leather materials (giving a measure of the layering of collagen fibrils in planes) and perpendicular to the surface of the tissue. For the edge on measurements a correlation is found between the tear strength and the OI. With a large number of samples of ovine and bovine leather a strong correlation is found between tear strength and a relatively small range of OI **[14]**. The ovine leather was selected on the basis of one group of low tear strength material (n = 15, with 228 diffraction patterns) and one group of higher strength material (n = 14, with 249 diffraction patterns) and one random group of bovine leather (n = 10, with 167 diffraction patterns). While the spread in OI values for each sample group is quite high (σ = 0.03, 0.03, 0.016 respectively) giving a low r^2 of 0.20 the fit is robust with a $p < 0.0001$ **(Fig. 4a) [14]**.

Taking a much smaller sample set, but with a much wider range of tear strengths, this time of leather from a range of different animal species, an extended correlation is found between tear strength and OI **[15]**. The leather from the mammals falls in a straight line with an r^2 of 0.98 and $p < 0.0001$ **(Fig. 4b).**

Acellular dermal matrix materials used for surgical scaffolds made from neonatal bovine dermis (5 months old), while stronger than their leather counterparts made from adult animals, also show a correlation between OI and tear strength **(Fig. 4d) [16]**.

If the strength is due to the sum of the components of the fibrils that lie in the direction of applied force then the OI is given by

$$OI = \frac{\int_0^{2\pi}\int_0^{\pi/2} \cos^4\theta \; F(\theta,\phi)\, d\theta\, d\phi}{\int_0^{2\pi}\int_0^{\pi/2} F(\theta,\phi)\, d\theta\, d\phi}$$

where $F(\theta,\phi)$ is the angular distribution function where θ and ϕ are orthogonal **[16]**.

While the structuring of collagen fibrils into a more layered structure may result in leather with higher tear strength, one may propose a thought experiment where this is extended to an OI =1 where the fibrils are perfectly aligned. Then there are no fibrils traversing layers and providing a strong fibre connection to tie the layers together. The connections between layers are then due only to the connections between fibrils. Connections in native tissues are generally believed to result from GAGs **[17-18]**, however these are known to be weak and recently this crosslinking effect has been challenged **[13, 19]**. In leather these GAGs have been removed and replaced by chromium or tannins, which are believed to form a similar role. Nevertheless, the bonds holding fibrils together are much weaker than the strength provided along the length of a fibril. Therefore, in a material where the fibrils are arranged perfectly in planes it might be imagined that the layers would separate. This has been identified, and it is known as looseness in leather.

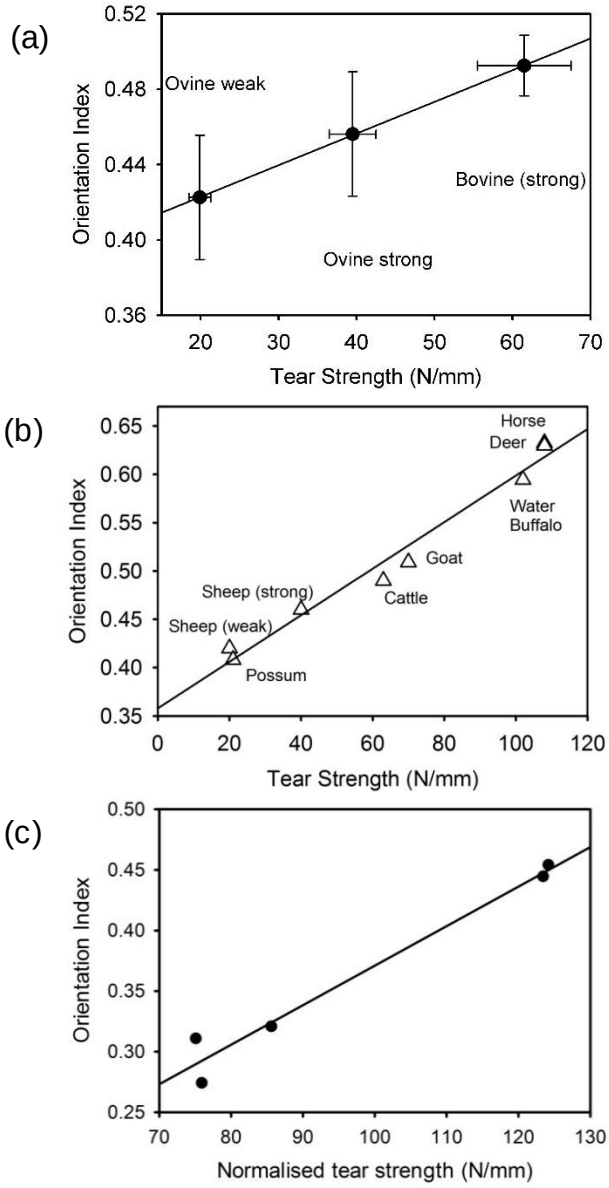

Fig. 4. Tear strength and OI for a) ovine and bovine leather, b) leather from a range of animals, c) bovine acellular dermal matrix for surgical scaffolds. a) adapted from Basil-Jones, M. M. et. al., *J. Agric. Food Chem.* **2011,** *59*, 9972, b) adapted from Sizeland, K. H. et. al., *J. Agric. Food Chem.* **2013,** *61*, 887, c) adapted from Wells, H. C. et. al., *ACS Biomat. Sci. Eng.* **2015,** *1*, 1026, with permission, all ©The American Chemical Society

Looseness may occur in bovine and other strong leather. Looseness is defined as the appearance of wrinkles on the surface (grain) of leather when it is folded grain side inwards. It is an undesirable attribute and results in a downgrade of the leather **[20]**. The OI through a cross section of tight (good) and loose (poor) leather

found that loose leather has a higher OI throughout the cross section **[21]**. The loose leather in this example also had a higher tear strength (130 ± 61 N mm^{-1} compared to 73 ± 10 N mm^{-1} for tight leather, with P <0.001 for the difference), in agreement with the correlation found between OI and tear strength in general for leather, but even with the higher strength the appearance of looseness substantially reduces the value of the leather. Looseness therefore is an example of a high OI continuing to increase strength but causing other undesirable properties. The correlation of strength and looseness with OI also provides a reason why looseness is mainly observed in leather from animals that typically produce high strength leather.

Age of donor animal and OI

The correlation between OI and tear strength in leather made from the skins of mammals also applies to other tissues. Pericardium, the membrane that encloses the heart and separates it from the other organs, is used in medical devices, especially in heart valve leaflet replacement. Pericardium is rich in type I collagen **(Fig. 2b, d)** and in contrast to collagen in dermis the collagen contains a strong crimp when not under tension. The strain at failure for bovine pericardium derived from neonatal animals is found to be 33 ± 4 MPa whereas from adult animals it is 19 ± 2 MPa. The stronger neonatal pericardium also has a higher OI, measured with X-rays edge on, of 0.78 compared with 0.63 for adult pericardium (with a $p < 0.0001$ for a comparison between these two OI values) **[22-23]**. The correlation between tear strength and OI is probably fairly universal for a range of tissue types, although the specific factors leading to high OI may vary.

Processing conditions

The structural arrangement of collagen fibrils in an animal derived material depends on both the native structure and also on the processing that the material has undergone. Changes that are caused by processing should be considered separately to those that occur naturally, in order to understand the inherent natural strength and the strength changes derived from processing conditions. Leather is prepared from skins through a series of processes to remove most non-collageneous components. This is followed by "cross linking" of the collagen with chromium or tannin followed by incorporation of fatliquors. Surgical scaffolds will typically be decellularised tissue with no cross linking agents or preservatives added. Heart valve leaflet replacements are normally decellularised tissue which has subsequently been treated with glutaraldehyde.

The OI varies during the stages of tanning from a salted skin (the normal starting material for a tannery) through to the dry crust staked (finished leather before the final stage of fatliquoring) **(Fig. 5).** While the variation in OI is quite large, so is the variation in thickness of the leather and of the moisture content. The OI can be adjusted for changes in thickness. If the materials containing a fibril expands in thickness uniformly, and the fibril is at an angle θ_1 from the base, then the new angle of the fibril, θ_2, depends on the change in thickness by:

$$\frac{T_2}{T_1} = \frac{\tan\theta_2}{\tan\theta_1}$$

where T1 is the original thickness, and T2 is the new thickness. Rearranging for θ_1 gives the new angle of the fibril after the leather has increased in thickness:

$$\theta_2 = \tan^{-1}\left(\frac{T_2}{T_1}\tan\theta_1\right)$$

Once corrected for thickness the remaining difference in OI is only due to water content with the wet samples having a higher OI (0.8 in the leather example) compared with dry leather (0.66) **[24]**.

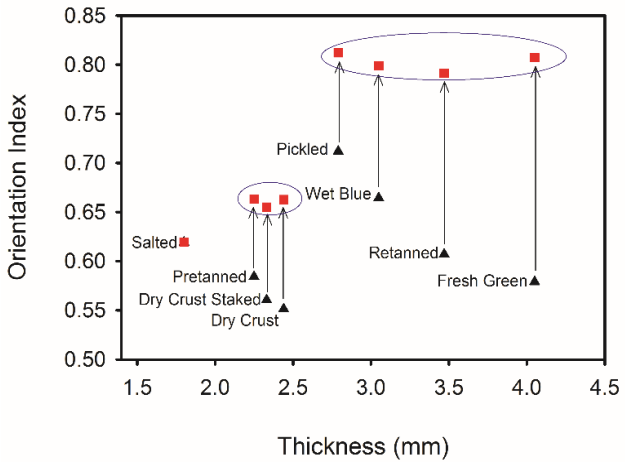

Fig. 5. Orientation index for skin during leather processing stages, thickness normalized. Reprinted with permission from Sizeland, K. H. et. al. *J. Agric. Food Chem.* **2015,** *63*, 2499 ©2015 The American Chemical Society.

Tissue adapting to strain

When collagen based materials are strained, the collagen fibrils respond to the strain in a number of ways. The collagen fibrils first reorient to the direction of strain **(Fig. 6a).** This is apparent in the shift in orientation of the features in the scattering pattern. The diffraction rings become centred on the direction of applied strain while the low q region of the pattern reflecting the form factor of collagen, importantly the fibril diameter, becomes aligned at right angles to this direction. As the orientation changes, the OI increases which is apparent as a narrowing of the azimuthal angle – intensity plot **(Fig. 6a) [12-13]**. This reflects the process of fibrils turning to the direction of applied strain, with those furthest from the direction of strain reorienting the most. In some materials such as pericardium (but not dermis) crimp may be present, and this is straightened in the early stages of stretching and reflected in both an increase in OI and an apparent decrease in fibril diameter (since the SAXS form factor gives an average diameter for the fibril). Finally the individual fibrils begin to stretch. This can be measured

by the increase in D-spacing, this change being directly proportional to the increase in length of the fibrils **(Fig. 6b)**. The fibril diameter, measured from SAXS as a tissue is strained, decreases at the same time as the D-spacing increases. These changes can be plotted together for a collagen material as it is strained **(Fig. 6c)**. From this, a Poisson's ratio for collagen fibrils can be calculated, which turns out to be large (2.1 ± 0.7) **[25]**. This variety of mechanisms for accommodating strain gives collagen materials great strength and toughness **[26-27]**.

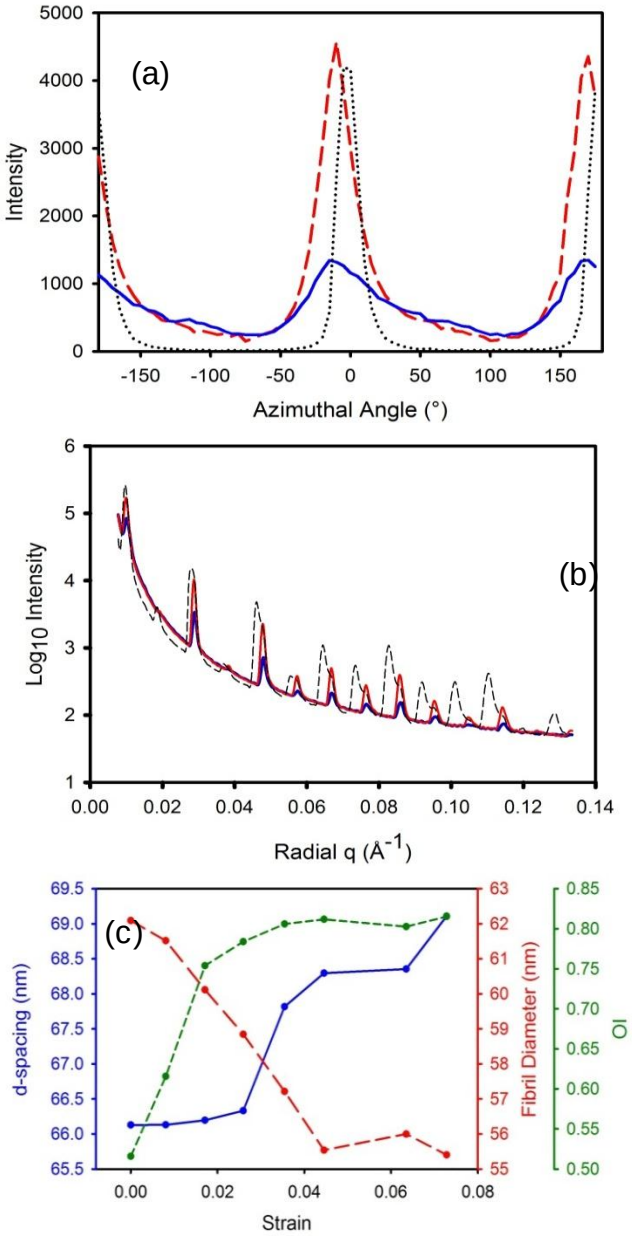

Fig. 6. Strained pericardium. (a) with strain the spread in azimuthal angle distribution decreases and centres on the direction of applied strain; (b) With increasing strain the D-spacing diffraction peaks shift; (c) fibril diameter, D-spacing and OI all change with strain. a) and b) Reprinted with permission from Kayed, H. R et.al. *RSC Adv.* **2015,** *5*, 103703 ©2015 The Royal Society of Chemistry; c) Reprinted with permission from Wells, H. C. et. al. *J. Appl. Phys.* **2015,** *117*, 044701 ©2015 The authors.

Conclusion

The arrangement of collagen fibrils in tissues has been characterized by synchrotron based small angle X-ray scattering supported by microscopy techniques. There was a strong correlation between tear strength, which is a good indicator of in-service performance, and the spread of fibril orientation (orientation index, OI). A highly layered structure provides the greatest tear strength. The OI of a natural material was found to depend on the individual source animal (with considerable variation between animals), the species of the source animal, the age of the animal, and processing conditions from the raw material to the finished product. The correlation between tear strength and OI appears to be universal for a range of tissue types. When collagen based materials are strained, the collagen fibrils respond to the strain by reorienting to the direction of strain with an increase in OI, then the individual fibrils begin to stretch. From this, a Poisson's ratio for collagen fibrils can be calculated. This variety of mechanisms for accommodating strain gives collagen materials great strength and toughness.

Acknowledgements

This work was supported by grants from the Ministry of Business Innovation and Employment LSRX0801 and LSRX1301 (MMB-J, KHS, HSW, SJRK), a Massey University Scholarship (HRK) a Royal Society of New Zealand NZ-Taiwan Nanotechnology Research Student Travel grant (HCW) and the Australian Synchrotron for travel funding and accommodation. Samples were provided by Southern Lights Biomaterails (NZ), TEI Biosciences (USA) and Tasman Tanning Ltd (NZ). This research was undertaken on the SAXS/WAXS beamline at the Australian Synchrotron, Victoria, Australia and the SAXS/WAXS beamline at NSRRC, Taiwan.

Author's contributions

Conceived the plan: RGH; Performed the experiments: HCW KHS HRK SJRK, MMB-J, RLE, RGH; Performed the data analysis: HCW KHS HRK SJRK, MMB-J, RLE, RGH; Wrote the paper: HCW, RGH. Authors have no competing financial interests.

References

1. Fratzl, P., *Collagen: Structure and mechanics*. Springer Science + Business Media: New York, 2008.
2. Badylak, S. F., *Biomaterials* **2007,** *28*, 3587. **DOI:** 10.1016/j.biomaterials.2007.04.043.
3. Vongpatanasin, W.; Hillis, L. D.; Lange, R. A., *N. Engl. J. Med.* **1996,** *335*, 407. **DOI:** 10.1056/nejm199608083350607.
4. Gautieri, A.; Vesentini, S.; Redaelli, A.; Buehler, M. J., *Nano Lett.* **2011,** *11*, 757. **DOI:** 10.1021/nl103943u.
5. Williams, J. M. V., *J. Soc. Leather Tech. Ch.* **2000,** *84*, 317.
6. Williams, J. M. V., *J. Soc. Leather Tech. Ch.* **2000,** *84*, 327.
7. ASTM, Standard Test Method for Bursting Strength of Textiles-Constant-Rate-of-Traverse (CRT) Ball Burst Test. 2011; pp 1.
8. Junqueira, L. C. U.; Bignolas, G.; Brentani, R. R., *Histochem. J.* **1979,** *11*, 447. **DOI:** 10.1007/bf01002772.
9. Fang, M.; Goldstein, E. L.; Turner, A. S.; Les, C. M.; Bradford, G. O.; Fisher, G. J.; Welch, K. B.; Rothman, E. D.; Banaszak Holl, M. M., *ACS Nano* **2012,** *6*, 9503. **DOI:** 10.1021/nn302483x.
10. Bigi, A.; Ripamonti, A.; Roveri, N.; Jeronimidis, G.; Purslow, P. P., *J. Mater. Sci.* **1981,** *16*, 2557. **DOI:** 10.1007/bf01113596.

11. Basil-Jones, M. M.; Edmonds, R. L.; Allsop, T. F.; Cooper, S. M.; Holmes, G.; Norris, G. E.; Cookson, D. J.; Kirby, N.; Haverkamp, R. G., *J. Agric. Food Chem.* **2010,** *58*, 5286. **DOI:** 10.1021/jf100436c.
12. Basil-Jones, M. M.; Edmonds, R. L.; Norris, G. E.; Haverkamp, R. G., *J. Agric. Food Chem.* **2012,** *60*, 1201. **DOI:** 10.1021/jf2039586.
13. Kayed, H. R.; Sizeland, K. H.; Kirby, N.; Hawley, A.; Mudie, S. T.; Haverkamp, R. G., *RSC Adv.* **2015,** *5*, 103703. **DOI:** 10.1039/C5RA21870E.
14. Basil-Jones, M. M.; Edmonds, R. L.; Cooper, S. M.; Haverkamp, R. G., *J. Agric. Food Chem.* **2011,** *59*, 9972. **DOI:** 10.1021/jf202579b.
15. Sizeland, K. H.; Basil-Jones, M. M.; Edmonds, R. L.; Cooper, S. M.; Kirby, N.; Hawley, A.; Haverkamp, R. G., *J. Agric. Food Chem.* **2013,** *61*, 887. **DOI:** 10.1021/jf3043067.
16. Wells, H. C.; Sizeland, K. H.; Kirby, N.; Hawley, A.; Mudie, S.; Haverkamp, R. G., *ACS Biomat. Sci. Eng.* **2015,** *1*, 1026. **DOI:** 10.1021/acsbiomaterials.5b00310.
17. Haverkamp, R. G.; Williams, M. A. K.; Scott, J. E., *Biomacromolecules* **2005,** *6*, 1816. **DOI:** 10.1021/bm0500392.
18. Scott, J. E., *J. Physiol-London* **2003,** *553*, 335. **DOI:** 10.1113/jphysiol.2003.050179.
19. Fessel, G.; Snedeker, J. G., *Matrix Biol.* **2009,** *28*, 503. **DOI:** 10.1016/j.matbio.2009.08.002.
20. Wells, H. C.; Holmes, G.; Haverkamp, R. G., *J. Sci. Food Agric.* **2016,** *96*, 2731. **DOI:** 10.1002/jsfa.7392.
21. Wells, H. C.; Holmes, G.; Jeng, U. S.; Wu, W.-R.; Kirby, N.; Hawley, A.; Mudie, S.; Haverkamp, R. G., *J Sci. Food Agric.* **2017,** *97*, 1549. **DOI:** 10.1002/jsfa.7899.
22. Kayed, H. R.; Sizeland, K. H.; Wells, H. C.; Kirby, N.; Hawley, A.; Mudie, S.; Haverkamp, R. G., *J. Biomat. Tissue Eng.* **2016,** *6*. **DOI:** 10.1166/jbt.2016.1532.
23. Sizeland, K. H.; Wells, H. C.; Higgins, J. J.; Cunanan, C. M.; Kirby, N.; Hawley, A.; Haverkamp, R. G., *BioMed Res. Int.* **2014,** *2014*, 189197. **DOI:** 10.1155/2014/189197.
24. Sizeland, K. H.; Edmonds, R. L.; Basil -Jones, M. M.; Kirby, N.; Hawley, A.; Mudie, S.; Haverkamp, R. G., *J. Agric. Food Chem.* **2015,** *63*, 2499. **DOI:** 10.1021/jf506357.
25. Wells, H. C.; Sizeland, K. H.; Kayed, H. R.; Kirby, N.; Hawley, A.; Mudie, S. T.; Haverkamp, R. G., *J. Appl. Phys.* **2015,** *117*, 044701. **DOI:** 10.1063/1.4906325.
26. Yang, W.; Sherman, V. R.; Gludovatz, B.; Schaible, E.; Stewart, P.; Ritchie, R. O.; Meyers, M. A., *Nat. Comm.* **2015,** *6*, 6649. **DOI:** 10.1038/ncomms7649.
27. Gupta, H. S.; Seto, J.; Krauss, S.; Boesecke, P.; Screen, H. R. C., *J. Struct. Biol.* **2010,** *169*, 183. **DOI:** 10.1016/j.jsb.2009.10.002.

